WARSAW UNIVERSITY OF TECHNOLOGY Index 351733
FACULTY OF CIVIL ENGINEERING
COMMITTEE FOR CIVIL AND WATER ENGINEERING
POLISH ACADEMY OF SCIENCES ISSN 1230-2945
DOI: 10.24425/ace.2024.150994
ARCHIVES OF CIVIL ENGINEERING
Vol. LXX ISSUE 3 2024
pp. 445 –457

Research paper

Application of BIM model based on improved region growth algorithm in building reinforcement and renovation

Cong Du[1], Yi Wen[2], Lijian Ren[3]

Abstract: In response to the current issue of poor modeling performance of Building Information Modeling for building models, a new Building Information Modeling based on an improved region growth algorithm is proposed. This method improves the region growth algorithm by introducing machine learning technology, and utilizes the improved algorithm to perfect the building model, thereby improving the efficiency of Building Information Modeling. The performance comparison experiment of the improved algorithm shows that its accuracy is 92.3%, respectively, which are lower than the comparison algorithm. Subsequent empirical analysis found that the robustness rating of the renovated building with the new Building Information Modeling was 94.06, significantly higher than the traditional model. The above results indicate that the new Building Information Modeling proposed in the study has high efficiency and accuracy in building reinforcement and renovation. This method can provide a new solution and idea for the field of building reinforcement and renovation.

Keywords: region growth algorithm, BIM model, building renovation, spherical fixed distance method, K-nearest neighbor method

[1]MSc., School of Civil Engineering, Inner Mongolia University of Technology, Hohhot, 010010, China, e-mail: ducong@imut.edu.cn, ORCID: 0009-0007-3368-7506

[2]MSc., College of Architecture, Inner Mongolia University of Technology, Hohhot, 010010, China, e-mail: wenyichina@126.com, ORCID: 0009-0005-9673-6454

[3]MSc., School of Civil Engineering, Inner Mongolia University of Technology, Hohhot, 010010, China, e-mail: renlijian0423@163.com, ORCID: 0000-0003-1629-4368

1. Introduction

The development of information technology and the arrival of the digital age are also causing significant changes in the construction industry [1]. Building Information Modeling (BIM) is a rapidly developing technique in recent years [2, 3]. It can present various links and processes of building engineering in a digital manner, making the design, construction, maintenance, and other aspects of building engineering more intelligent and efficient. In the field of building reinforcement and renovation, BIM has become an important tool and means [4]. At present, the application of BIM in building reinforcement and renovation mainly focuses on two aspects: firstly, using BIM models to design, construct, and maintain buildings; The second is engineering management based on the BIM model, which utilizes the BIM model for building operation management and maintenance [5]. However, there are still some problems and challenges in the application of BIM in building reinforcement and renovation [6]. For example, due to differences in design and construction standards among different regions and building types, it is difficult for BIM to be effectively applied in design and construction; In addition, the current BIM has the problem of information silo, which leads to the inability to effectively integrate and share information. Therefore, to solve the above problems, this article studies the application of a BIM model combined with an improved region growth algorithm in building reinforcement and renovation, thus providing a new solution and idea for the field of building reinforcement and renovation.

2. Related works

With the widespread application of 3D laser scanning technology in construction projects, region growth algorithms (RGA) and point cloud plane extraction algorithms (PCPE) have received high attention. Pan et al. put forward a crystal region dynamics mode combining temperature cycling with RGA to solve the problem of size dependence during crystal crystallization, and conducted empirical research on it. Finally, it was found that this model can reduce the sensitivity of crystal size in crystal crystallization compared to traditional methods [7]. To accurately monitor the profile of steel bars, Robert et al. proposed a steel bar planar contour algorithm based on automatic non parametric principle. Empirical analysis shows that this algorithm significantly improves the accuracy of steel bar contour detection compared to traditional algorithms [8]. To improve the charging efficiency of charging devices on the plane, Wang led his team to propose a dominating coverage set extraction algorithm. Through effectiveness verification, it was found that the average performance of this algorithm is at least 33.49% higher than that of the comparison algorithm, and it has practical application value [9]. To solve the problem that it is difficult to monitor the physical defects in organic solar cell, Sciuto et al. proposed to combine the elliptic basis function neural network with the moment extraction algorithm to build a recognition model for the physical defects of cells. The analysis of this model shows that its classification accuracy in the test dataset is 89.3%, indicating its effectiveness [10]. Liu et al. designed an accurate point set registration method on feature fusion to address the issue of excessive noise in point cloud data. This method has been

empirically studied in orthodontic scenarios and has been concluded to be more effective than traditional methods in registration, achieving the goal of noise reduction in cloud point data [11].

With the increasing regularity and complexity, research on optimizing BIM models is also increasing. To improve the effectiveness of construction project decision-making, Tavakolan et al. proposed integrating ontology knowledge with semantic reasoning technology to construct a building planning information collection and decision support system. This system can effectively improve the planning level of decision-makers [12]. To understand the evaluation of BIM by construction professionals, Olanrewaju et al. proposed combining the obstacles to BIM implementation with questionnaire survey methods to construct a descriptive analysis plan for BIM evaluation. Empirical experiments have shown that construction professionals believe it can be used to develop appropriate mitigation solutions [13]. To prevent health project costs from exceeding standards, Meisaroh et al. constructed a BIM based on the quantity takeoff algorithm. The important factors in the cost of health projects are drawings, project quantities and interoperability of data. It is also found that the cost-benefit of this model for health construction projects is as high as 5.34% [14]. To address the issue of insufficient digitization of construction project planning processes and information, Walter led his team to combine BIM with open data exchange technology to construct a digital model for building applications. This model completes the digitization and sharing of building information, which can be used for future evaluation and testing [15]. To improve the accuracy of heat and cooling load calculation data, Lawson proposed a load calculation scheme based on BIM technology. This scheme can eliminate common errors in traditional calculation schemes and significantly improve the accuracy of load calculation results [16].

In summary, with the rise of the building renovation craze, there is increasing attention to RGA and BIM. And currently, many improved methods have been applied to RGA and BIM technologies, but there are still few studies combining RGA and BIM technologies. Therefore, this study combines RGA and BIM technology to construct a BIM model that combines RGA, aiming to perfect the accuracy and validity of building information collection and provide auxiliary support for rational planning of building resources.

3. Application of BIM model based on improved RGA in building reinforcement and renovation

3.1. PCPE based on region growth

RGA is an image segmentation method that uses a minimum spanning tree to achieve image segmentation, effectively extracting images from the target area while avoiding excessive image segmentation [17]. In building reinforcement and transformation, the application of area growth algorithm mainly relies on image processing technology to realize the segmentation and identification of the building surface by processing and analyzing the surface data of the building. Although the area growth algorithm mainly deals with plane graphics, it can be processed on a two-dimensional plane by transforming the surface of the building into image data, so it can be applied to building reinforcement transformation. At the same time the

research object of building reinforcement and renovation application is a simple plane model, and PCPE can accurately extract flat surfaces, such as ground, plane, and facade information from the point cloud data (PCD) [18]. Therefore, the study combined RGA with PCPE to construct a PCPE based on region growth. Fig. 1 shows the structural diagram of this algorithm.

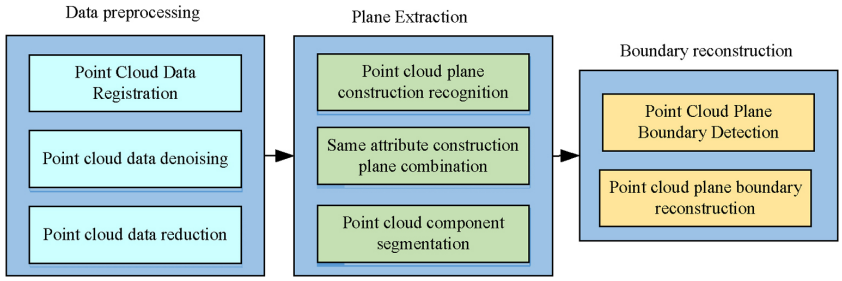

Fig. 1. PCPE algorithm based on region growth

Fig. 1 shows the PCPE flowchart based on region growth. The process includes the collection and processing of PCD, point cloud plane cutting, plane boundary detection and reconstruction, plane type recognition, point cloud plane construction with the same attribute, and point cloud construction segmentation process [19]. The plane extraction of point clouds involves dividing the points in the point cloud into different point sets based on the same plane. The directly collected PCD is usually in a disorderly and diverse state, so research first needs to preprocess the PCD, including PCD registration, PCD denoising, and PCD reduction. Firstly, PCD of buildings is collected through laser scanning technology; Subsequently, point cloud data is registered, which involves matching and aligning the local coordinate system of the collected PCD with the common global coordinate system to achieve complete PCD collection. The second step is point cloud denoising. As a result of the fact that the PCD collected by the laser scanner contains noise that is not needed for research, such as moving objects, surrounding environment, and reflection artifacts. Therefore, research is conducted on denoising the registered point cloud data through grid and scattered point cloud denoising techniques. After denoising, PCD will still have the characteristics of massive data and dense point clouds. In response to this phenomenon, research has been conducted on simplifying PCD through triangular patch simplification and direct simplification methods. Fig. 2 is a simplified processing step diagram.

As Fig. 2, in the simplification step, the point cloud data will first be imported into the 3D spatial coordinate system and voxelated using a uniform grid; After determining the size of voxel mesh parameters, a simplification operation of cloud point data is attempted by eliminating all cloud points in the same voxel. After processing the collected point cloud data, point cloud plane extraction is performed on the point cloud data through RGA. Region growth is an algorithm that combines point cloud data with similar properties to achieve point cloud region merging [20]. Combining the K-nearest neighbor method and the spherical fixed distance method plays an important role in regional growth point cloud planar cutting. These two methods enable more precise classification and boundary optimization, thus improving the accuracy and

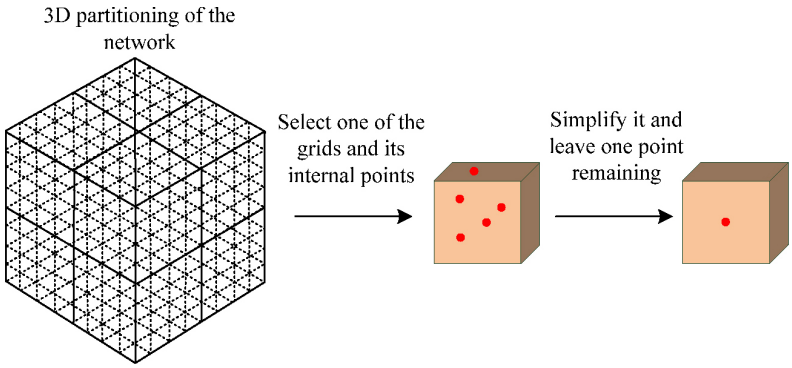

Fig. 2. Cloud data reduction processing steps

efficiency of the cut. Through the steps of initial classification, determining seed points, region growing, boundary optimization, executing cuts, and result evaluation and adjustment, it can satisfy a variety of complex point cloud data cutting scenarios and meet the needs of different applications. By using the spherical fixed distance method and K-nearest neighbor method to search for adjacent points of each cloud point, seed points are established and growth points are selected based on this, achieving the extraction of segmentation planes for cloud point sets. Subsequently, perform plane fitting on the segmented point set and match the specific plane model with the segmented point cloud [21]. By obtaining the optimal plane parameters, the overlap between point cloud data and model parameters can be achieved. The study uses the least squares method to find the plane with the smallest distance from the segmented plane, and the fitting Equation of the center of gravity of the cloud point is obtained from Eq. (3.1).

$$ax + by + cz = d \tag{3.1}$$

In Eq. (3.1), x is the horizontal coordinate of each point in the plane; y is the vertical coordinate of each point in the plane. The sum of the distances between the desired plane and the segmented plane point cloud is defined as o, and the plane with the lowest o value is the cloud point fitting plane. The calculation equation for o is Eq. (3.2).

$$o = \sum_{i=1}^{n} \frac{\left(a_{x_i} + b_{y_i} + c_{z_i} - d\right)^2}{a^2 + b^2 + c^2} \tag{3.2}$$

In Eq. (3.2), x_i is the abscissa of point cloud P_n; y_i is the ordinate of point cloud P_n; z_i is the vertical coordinate of point cloud P_n. All points in a plane equation are in the same plane, and the coefficients multiplied by their horizontal, vertical, and vertical coordinates can be any number, but each coefficient cannot be zero at the same time. Therefore, the plane equation must have constraints, and the calculation equation for the constraints is Eq. (3.3).

$$\begin{cases} a^2 + b^2 + c^2 = 1 \\ a\overline{x} + b\overline{y} + c\overline{z} = d \end{cases} \tag{3.3}$$

In Eq. (3.3), $\overline{x}$ means the abscissa of the point; $\overline{y}$ represents the ordinate of the center point; $\overline{z}$ is the VC of the center point. The objective function of the least squares method is Eq. (3.4).

$$F = \min\left(\sum_{i=1}^{n}(a(x_i-\overline{x})+b(y_i-\overline{y})+c(z_i-\overline{z}))\right) \tag{3.4}$$

Eq. (3.4) is the same as Eq. (3.3). The cloud point and the distance matrix of the fitting surface are defined, and the matrix equation is Eq. (3.5).

$$AX = \begin{bmatrix} x_1-\overline{x}, y_1-\overline{y}, z_1-\overline{z} \\ x_2-\overline{x}, y_2-\overline{y}, z_2-\overline{z} \\ \cdots \\ x_n-\overline{x}, y_n-\overline{y}, z_n-\overline{z} \end{bmatrix}, \quad \begin{bmatrix} a \\ b \\ c \end{bmatrix} = \begin{bmatrix} a(x_1-\overline{x})+b(y_1-\overline{y})+c(z_1-\overline{z}) \\ a(x_2-\overline{x})+b(y_2-\overline{y})+c(z_2-\overline{z}) \\ \cdots \\ a(x_n-\overline{x})+b(y_n-\overline{y})+c(z_n-\overline{z}) \end{bmatrix} \tag{3.5}$$

Eq. (3.5) is similar to both of Eq. (3.3) and (3.4). At this point, the minimum function equation of the least squares method is Eq. (3.6).

$$\begin{cases} \|AX\| = \sqrt{\sum_{i=1}^{n}((x_2-\overline{x})+b(y_2-\overline{y})+c(z_2-\overline{z}))^2} \\ F = \min\sum_{i=1}^{n}((x_2-\overline{x})+b(y_2-\overline{y})+c(z_2-\overline{z}))^2 \end{cases} \tag{3.6}$$

The equation for singular value decomposition of matrix A is Eq. (3.7).

$$\begin{bmatrix} x_1-\overline{x}, y_1-\overline{y}, z_1-\overline{z} \\ x_2-\overline{x}, y_2-\overline{y}, z_2-\overline{z} \\ \cdots \\ x_n-\overline{x}, y_n-\overline{y}, z_n-\overline{z} \end{bmatrix} = UVD \tag{3.7}$$

In Eq. (3.7), D represents the diagonal matrix. U and V represent unitary matrices. After obtaining the fitting plane of the point set, projecting the 3D-point-cloud into the fitting base surface, and a 2D coordinate system is established based on this to achieve the conversion step of the 2D point set. Define the segmented point cloud as P_n, and the projection on the fitting plane as P'_n, P_n, and P'_n as defined in Eq. (3.8).

$$P_n = \begin{bmatrix} x_1, y_1, z_1 \\ x_2, y_2, z_2 \\ \cdots \\ x_n, y_n, z_n \end{bmatrix}, \quad P'_n = \begin{bmatrix} x'_1, y'_1, z'_1 \\ x'_2, y'_2, z'_2 \\ \cdots \\ x'_n, y'_n, z'_n \end{bmatrix} \tag{3.8}$$

Eq. (3.9) is the equation for calculating the distance of projection.

$$\left|P_iP'_i\right| = \frac{|ax_i+by_i+cz_i-d|}{\sqrt{a^2+b^2+c^2}} = |ax_i+by_i+cz_i-d| \tag{3.9}$$

Eq. (3.10) is the calculation equation for the coordinate of the projection point P_i'.

$$\begin{cases} t = |ax_i + by_i + cz_i - d| \\ x_i' = x_i - at \\ y_i' = y_i - bt \\ z_i' = z_i - ct \end{cases} \tag{3.10}$$

Subsequently, the 3D projection points are converted into 2D. Firstly, to establish a coordinate system and define the first projection point P_1' as the origin of the 2D coordinate system; The direction from the first projection point to the second projection point is derived as the positive abscissa direction. This XOY two-dimensional coordinate system is established. Eq. (3.11) is the vector equation for the horizontal coordinate system.

$$P_1'P_2' = (x_2' - x_1', y_2' - y_1', z_2' - z_1') \tag{3.11}$$

(x_1', y_1', z_1') and (x_2', y_2', z_2') are the 3D coordinate of the projection point p_1' and p_2'. Define the i-th point as P_i', and if the $P_1'P_i'$ and X axes are square, then the angle between $P_1'P_i'$ and $P_1'P_i'$ is θ. The equation for calculating the sine and cosine of θ is Eq. (3.12).

$$\cos\theta = \frac{P_1'P_i' \cdot P_1'P_2'}{\left|P_1'P_i'\right| \cdot \left|P_1'P_2'\right|} \tag{3.12}$$

The calculation equation for the 2D point P_i'' corresponding to P_i' is Eq. (3.13).

$$\begin{cases} x_i^n = \left|P_1'P_i'\right| \cdot \cos\theta \\ y_i^n = \left|P_1'P_i'\right| \cdot \sin\theta \end{cases} \tag{3.13}$$

Finally, by using region based growth α-shapes algorithm, the 2D point set boundaries are extracted and reconstructed to obtain the required building data.

3.2. Application of new BIM model in building renovation

BIM is a digital expression data model that aggregates information related to construction projects through digital technology, which can improve the efficiency, quality, and sustainability of construction projects. The study integrates the region growth based plane extraction algorithm with traditional BIM models to construct a BIM model based on region growth plane extraction. After processing the spatial plane point cloud data, it is vital to identify the PCD of building components in the plane data. The construction recognition process is divided into construction type recognition and construction geometry information recognition. Due to the use of laser scanning technology to collect and preprocess PCD, it only represents the entire building and does not differentiate the components within the building. Therefore, the study uses geometric features and topological network algorithms to extract features from planar point cloud data, achieving type recognition of building components. Calculates the normal direction of the plane through cosine values. The angle between the normal vector of the segmentation plane and (0,0,1) is defined as θ', and the judgment equation is Eq. (3.14).

$$\cos\theta' = \frac{(a,b,c)\cdot(0,0,1)}{\sqrt{a^2+b^2+c^2}} = c = \begin{cases} 0, & \text{horizontal plane} \\ 1, & \text{vertical plane} \end{cases} \tag{3.14}$$

In Eq. (3.14), if the plane is judged as a horizontal plane, it may be the plane of the plate and the bottom surface of the beam; If the plane is judged as an elevation, it may be the side of the beam, the wall mounting surface, and the column elevation. Subsequently, feature judgment on the contour of the plane is performed, and the judgment equation is Eq. (3.15).

$$\frac{x_{\max}}{y_{\max}} \begin{cases} > 2.5, & \text{beam sides} \\ < 0.4, & \text{columns, sides} \\ \approx 1, & \text{wall facade} \end{cases} \tag{3.15}$$

In Eq. (3.15), $x_{\max}$ is the maximum horizontal side length of the plane; $y_{\max}$ is the maximum vertical side length of the plane. In actual engineering, the judgment accuracy of only constructing through Eq. (3.15) is insufficient. The study uses the length of the vertical side as the basis for judgment. If the length of the vertical side is close to the height of the floor, it is the wall facade, and if it is shorter, it is the side of the beam. If the plane is a horizontal plane, the longest edge in the vertical contour direction is recorded as length and width; If the aspect ratio is not large, it is a plate, and if the aspect ratio is large, it is a column. However, geometric features cannot identify door and window voids, and recognition errors are prone to occur. It is necessary to verify the topological relationship to ensure accurate and accurate recognition of plane types. After achieving type recognition of point cloud planes, geometric segmentation of components with the same attributes is performed, and the attribute segmentation standards are demonstrated in Table 1.

Table 1. Attribute segmentation criteria

Code	Plane type	Judgment rules
A1	Cylinder	Common contour edges exist perpendicular to each other
A2	Beam surface	Common contour edges exist perpendicular to each other
A3	Board surface	Parallel to each other, with small distances between planes and similar coordinate ranges between planes
A4	Metope	Parallel to each other and with small distances between planes, the horizontal projection length range is close

In Table 1, the plane can be judged by the dot product of its fitting plane's unit normal vector, and the judgment equation is Eq. (3.16).

$$n_1 \cdot n_2 = (a_1, b_1, c_1) \cdot (a_2, b_2, c_2) \approx \begin{cases} 0, & \text{vertical} \\ \pm 1, & \text{parallel} \end{cases} \tag{3.16}$$

After completing the identification of component types and geometric information, the BIM model is constructed based on relevant information and topological relationships. The required parameters include the geometric parameters of component beams, slabs, columns, walls, doors, and windows. The geometric parameters of the beam are the top height of the beam, the starting and ending points of the beam centerline, the beam height, and the beam width; The geometric

parameters of the plate are the boundary of the plate contour and the thickness of the plate; The columns are the height of the column base, the height of the column top, the width of the column, and the depth of the column; The wall is the height of the wall bottom and the wall top, the starting and ending points of the wall centerline, the wall thickness, and the wall contour line; The is are the coordinates of the door, the height of the door bottom, the width and height of the door; Windows is window coordinates, window bottom elevation, window width, and window height. The above parameters will be developed through software Revit2016 for secondary programming to improve parameter information. The programming language for secondary development is C#, and the programming steps are divided into the creation of elevations, slab markers, walls, and columns, beams, and doors and windows. Set the elevation through the CreateLevel function. Public Floor NewSlab sets floorslab; Profile sets the floor profile; SlopedArrow sets the slope, Public Walls Create sets the wall height, wall type (thickness), and position; FamilyInstance sets the coordinates, length, width, and elevation of columns, columns, doors, and windows. After the BIM parameters are determined and the BIM is built in the above way, the new BIM model will be used to build the architectural model that needs to be reconstructed and strengthened. In this way, the architectural model can be strengthened and reconstructed better, so as to sustainably accelerate developing the construction industry.

4. Interpretation of result

4.1. Comparative analysis of improved RGA performance

In order to test and analyze the actual performance of the proposed Improved Region Growth Algorithm (IRGA), the study compares its performance with that of Region Split and Merge (RSM), Feature Pyramid Network (FPN) and Random Sample Consensus (RANSAC) based extraction algorithms. Machine (FPN) and Random Sample Consensus (RANSAC) based extraction algorithms. The research takes the accuracy, loss rate, precision rate, recall rate, PR curve, selection rate, and consumption time of the algorithm as comparative indicators, and verifies them in the ABW public dataset. The experimental environment for this study is as follows: the development environment is VC++software, the development framework is MFC class library, the graphics library is OPENGL, and the PC set is 2.2 GHz, 2.0 GB. The accuracy and loss rate results of the four algorithms are displayed in Fig. 3.

From Fig. 3(a), it is evident that as the iterations increases, the accuracy of all four algorithms shows an increasing trend, and the loss rate of them shows a decreasing trend. In the comparison of the accuracy curves of the four algorithms, it can be found that the IGRA tends to stabilize with an accuracy of 92.3%, which is higher than RANSAC's 86.7%, FPN algorithm's 85.1%, and RSM algorithm's 84.9%. In addition, the loss rate comparison curve in Fig. 3(b) shows that the final loss rate of IGRA is 2.35%, lower than RANSAC's 2.41%, FPN's 2.48%, and RSM's 2.52%. The above results indicate that from the dimensions of accuracy and loss rate, IGRA performs better than other comparative algorithms. Fig. 4 shows the accuracy and average absolute error results.

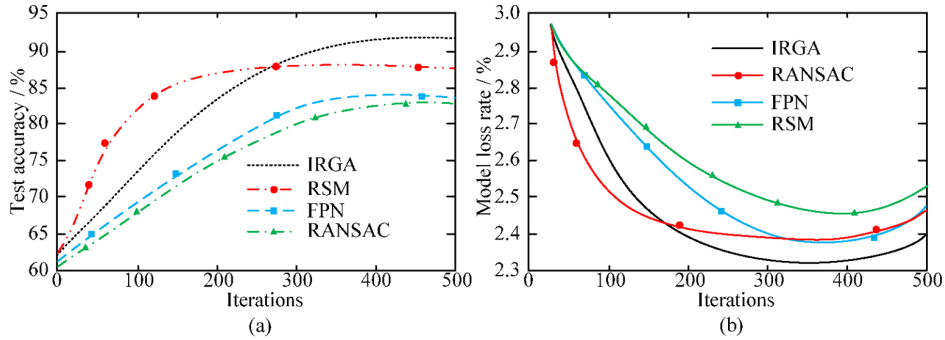

Fig. 3. Comparison of accuracy and loss rate results of four algorithms; (a) Comparative accuracy results of the four methods, (b) Comparative results of loss values for four methods

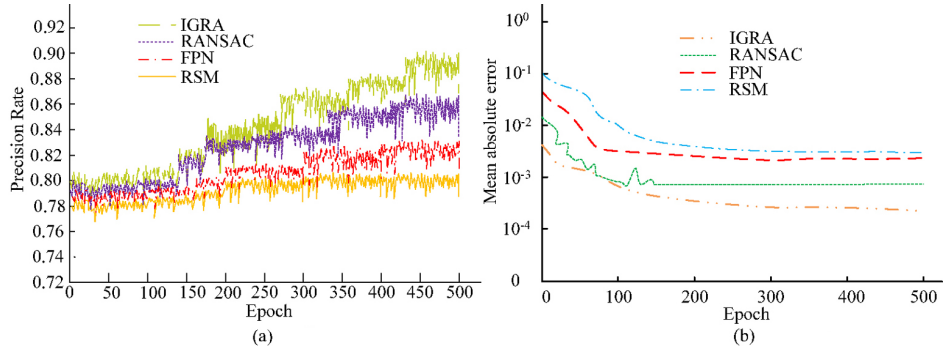

Fig. 4. Accuracy and average absolute error results of four algorithms; (a) Precision rate, (b) Mean absolute error

Fig. 4(a) is the comparison of the four algorithms' accuracy: as the iterations increases, the accuracy of all four algorithms shows an increasing trend. The accuracy of IGRA towards stability is 95.6%, which is higher than RANSAC's 91.8%, FPN's 89.6%, and RSM's 88.6%. Fig. 4(b) shows the comparison of the average absolute error: with the increase of iterations, the average absolute error of the four algorithms shows a downward trend. The average absolute error of IGRA tending to be stable is 0.00056, which is higher than 0.00075 of RANSAC, 0.0078 of FPN and 0.0081 of RSM. The above data verify that the IGRA performance is better than that of the comparison algorithm in terms of accuracy and average absolute error. Fig. 5 shows the selection rates and PR curve results of the four algorithms.

As the graph of the PR curves in Fig. 5 of the four algorithms: the PR curves of all four algorithms show a downward trend. The area under the PR curve of the IGRA algorithm is 0.91, which is higher than RANSAC's 0.85, FPN's 0.83, and RSM's 0.79. Fig. 5(b) shows the comparison results of image selection rates among the four algorithms. The study repeated six experiments to prevent accidental errors. In Fig. 5(b), the IGRA algorithm has the highest image selection rate among the four algorithms in all six experiments. And its average image selection rate is 95.6%, which is higher than 90.6% of RANSAC, 88.6% of FPN, and 86.9%

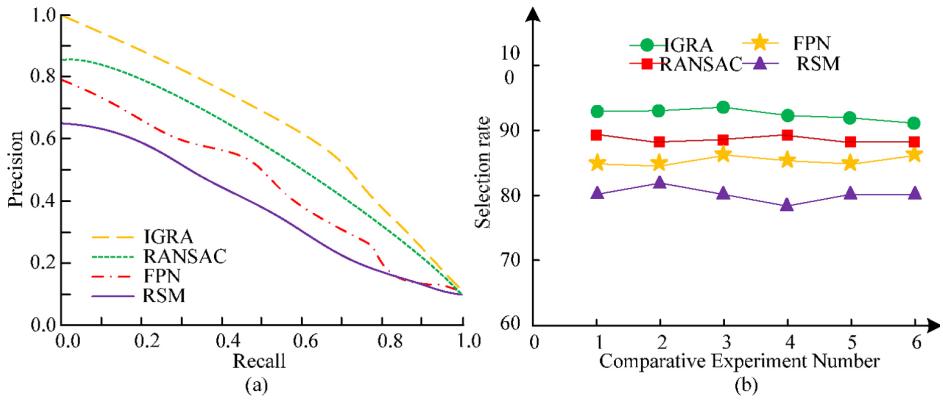

Fig. 5. Comparison results of selection rate and PR curve of four algorithms; (a) PR curve, (b) Selection rate comparison results

of RSM. The above results indicate that from the dimensions of image selection rate and PR curve, the performance of the IGRA algorithm proposed in the study is superior to similar RANSAC algorithm, FPN algorithm, and RSM algorithm.

4.2. Empirical analysis of a new BIM model

After comparing the IGRA algorithm, to analyze the new BIM performance based on the IGRA, the study simulated room point cloud data using Matlab software, with size $3 \times 3 \times 6$ m. Implement the automatic generation of a new BIM model by importing component algorithms and component extraction parameters into the Revit secondary development program. To analyze the practical application effect of the new BIM in building renovation and reinforcement, this study aiming applies the new BIM to the actual renovation and reinforcement process of a certain building. This study uses a new BIM model and a traditional BIM model to model buildings in the same batch that need to be renovated and reinforced, and based on this, proposes suggestions for renovation and reinforcement. After the renovation of the building, the study analyzed the practical application effects of new BIM models and traditional BIM models using professional evaluators' evaluation scores for the robustness of the building's renovation. The study divided professional evaluators into four groups and rated the robustness of buildings reconstructed based on two BIM models, as shown in Fig. 6.

From Fig. 6, it can be seen that the four groups of professional judges rated the robustness of buildings reconstructed based on the new BIM model higher than those reconstructed based on the traditional BIM model. And the average score of the four groups of evaluators on the robustness of buildings reconstructed based on the new BIM model is 94.06 points, significantly higher than the 86.61 points of the four groups of evaluators on the robustness of buildings reconstructed based on the new BIM model. The above results indicate that using a new BIM model to construct a model and reinforcing the building on this basis has a better effect on enhancing the robustness of the building than traditional BIM models.

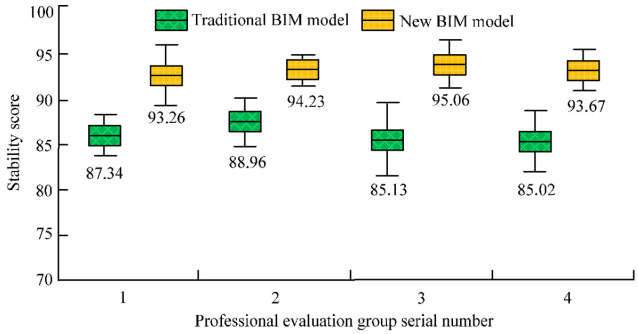

Fig. 6. Comparison of building durability scores between two BIM models

5. Conclusions

To improve the construction accuracy of BIM in the construction of architectural model, this study combines spherical fixed distance method and K nearest neighbor method with RGA to obtain the IGRA algorithm. On the basis of this algorithm, a new BIM model is built, hoping that the new BIM model can more accurately build the architectural model. This study compares the performance of IGRA with RANSAC, FPN algorithm, and RSM algorithm. The accuracy of IGRA was found to be 92.3%, which is higher than the RANSAC algorithm's 86.7%, NS algorithm's 85.1%, and RSM algorithm's 84.9%. Subsequently, empirical analysis of the new BIM model showed that the rating for the robustness of the reconstructed building based on the new BIM model was 94.06 points, much higher than the 86.61 points of the traditional BIM model. The above results indicate that using a new BIM model with improved RGA can effectively improve the quality and efficiency of building reinforcement and renovation plans. Matlab software is not a professional point cloud processing platform, and PCL professional point cloud processing platform needs to be used for analysis in the future to improve the efficiency of point cloud processing.

Acknowledgements

The research is supported by: First-class Curriculum Project of Inner Mongolia Autonomous Region-Professional Innovation Practice-Principle and Application of BIM Technology.

References

[1] N. Shakeel and S. Shakeel, "Context-free word importance scores for attacking neural networks", *Journal of Computational and Cognitive Engineering*, vol. 1, no. 4, pp. 187–192, 2022, doi: 10.47852/bonviewJCCE2202406.

[2] A. Miatto, C. Sartori, M. Bianchi, P. Borin, A. Giordano, and S. Saxe, "Tracking the material cycle of Italian bricks with the aid of building information modeling", *Journal of Industrial Ecology*, vol. 26, no. 2, pp. 609–626, 2022, doi: 10.1111/jiec.13208.

[3] W. Trochmiak, A. Krygier, M Stachura and J. Jaworski, "The BIM 5D model of the bridge built usingthe incremental launching method", *Archives of Civil Engineering*, vol. 69, no. 3, pp. 157–172, 2023, doi: 10.24425/ace.2023.146073.

[4] M. Najjar, K. Figueiredo, A. Hammad, and A. Haddad, "Integrated optimization with building information modeling and life cycle assessment for generating energy efficient buildings", *Applied Energy*, vol. 250, no. 15, pp. 1366–1382, 2019, doi: 10.1016/j.apenergy.2019.05.101.

[5] H. Liu, J. Song, and G. Wang, "Development of a tool for measuring building information modeling (BIM) user satisfaction-method selection, scale development and case study", *Engineering, Construction and Architectural Management*, vol. 27, no. 9, pp. 2409–2427, 2020, doi: 10.1108/ECAM-08-2019-0448.

[6] B. Koo, S. La, N.W. Cho, and Y. Yu, "Using support vector machines to classify building elements for checking the semantic integrity of building information models", *Automation in Construction*, vol. 98, pp. 183–194, 2019, doi: 10.1016/j.autcon.2018.11.015.

[7] H.J. Pan and J.D. Ward, "Computationally efficient algorithm for solving population balances with size-dependent growth, nucleation, and growth-dissolution cycles", *Industrial and Engineering Chemistry Research*, vol. 60, no. 34, pp. 12614–12628, 2021, doi: 10.1021/acs.iecr.1c01947.

[8] S.R. Anderson, V.P. Debattista, P. Erwin, et al., "The secular growth of bars revealed by flat (peak + shoulders) density profiles", *Monthly Notices of the Royal Astronomical Society*, vol. 513, no. 2, pp. 1642–1661, 2022, doi: 10.1093/mnras/stac913.

[9] X. Wang, H. Dai, W. Wang, J. Zheng, N. Yu, G. Chen, W. Dou, and X. Xu, "Practical heterogeneous wireless charger placement with obstacles", *IEEE Transactions on Mobile Computing*, vol. 19, no. 8. pp. 1910–1927, 2020, doi: 10.1109/TMC.2019.2916384.

[10] G.L. Sciuto, G. Capizzi, R. Shikler, and C. Napoli, "Organic solar cells defects classification by using a new feature extraction algorithm and an EBNN with an innovative pruning algorithm", *International Journal of Intelligent Systems*, vol. 36, no. 6, pp. 2443–2464, 2021, doi: 10.1002/int.22386.

[11] Y. Liu, S. Du, W. Cui, et al., "Precise point set registration based on feature fusion", *The Computer Journal*, vol. 64, no. 7, pp. 1039–1055, 2021, doi: 10.1093/comjnl/bxab114.

[12] M. Tavakolan, S. Mohammadi, and B. Zahraie, "Construction and resource short-term planning using a BIM-based ontological decision support system", *Canadian Journal of Civil Engineering*, vol. 48, no. 1, pp. 75–88, 2021, doi: 10.1139/cjce-2019-0439.

[13] O.I. Olanrewaju, N. Chileshe, S.A. Babarinde, and M. Sandanayake, "Investigating the barriers to building information modeling (BIM) implementation within the Nigerian construction industry", *Engineering, Construction and Architectural Management*, vol. 27, no. 10, pp. 2931–2958, 2020, doi: 10.1108/ECAM-01-2020-0042.

[14] M. Meisaroh, A.E. Husin, and B. Susetyo, "Analysis of key success factors using RII method on the implementation building information modeling (BIM)-based quantity take-off to improve cost performance hospital structure", *Solid State Technology*, vol. 64, no. 2, pp. 3179–3188, 2021.

[15] J. Walter, T. Obermeier, and J. Díaz, "BIM in der brandschutzplanung: praxisrelevante attribute und klassen/BIM in fire protection planning: Attributes and classes relevant to practice", *Bauingenieur*, vol. 96, no. 5, pp. 182–190, 2021, doi: 10.37544/0005-6650-2021-05-66.

[16] K. Lawson, "Validating BIM load calculations", *ASHRAE Journal*, vol. 7, no. 64, pp. 30–35, 2022.

[17] H.J. Pan and J.D. Ward, "Computationally efficient algorithm for solving population balances with size-dependent growth, nucleation, and growth-dissolution cycles", *Industrial and Engineering Chemistry Research*, vol. 60, no. 34, pp. 12614–12618, 2021, doi: 10.1021/acs.iecr.1c01947.

[18] F. Tang, "An improved intelligent bionic optimization algorithm based on the growth characteristics of tree branches", *Journal of Intelligent and Fuzzy Systems*, vol. 40, no. 3, pp. 3821–3829, 2021, doi: 10.3233/JIFS-190487.

[19] S.R. Anderson, V.P. Debattista, P. Erwin, et al., "The secular growth of bars revealed by flat (peak + shoulders) density profiles", *Monthly Notices of the Royal Astronomical Society*, vol. 512, no. 2, pp. 1642–1661, 2022, doi: 10.1093/mnras/stac913.

[20] S. Sun, M. Jiang, D. He, Y. Long, and H. Song, "Recognition of green apples in an orchard environment by combining the GrabCut model and Ncut algorithm", *Biosystems Engineering*, vol. 187, pp. 201–213, 2019, doi: 10.1016/j.biosystemseng.2019.09.006.

[21] C. Kampen, B.N. Mckinley, and J.R. Dan, "Building information modeling project coordination: The all-in approach", *Pci Journal*, vol. 66, no. 1, pp. 22–27, 2021, doi: 10.15554/pcij66.1-03.

Received: 2023-11-10, Revised: 2024-01-23